Journal of Ceramic Processing Research. Vol. 14, No. 5, pp. 632~635 (2013)

J O U R N A L O F
Ceramic Processing Research

Effect of annealing on the electrochromic properties of WO_3 thin films fabricated by electrophoretic deposition

Yoon-Tae Park[a] and Ki-Tae Lee[a,b]*

[a]*Division of Advanced Materials Engineering, Chonbuk National University, Jeonbuk 561-756, Korea*
[b]*Hydrogen and Fuel Cells Research Center, Chonbuk National University, Jeonbuk 561-756, Korea*

WO_3 thin films were fabricated by an electrophoretic deposition (EPD) process. As-deposited WO_3 thin films was annealed at 100 °C for 24 hrs to improve the electrochromic properties with better cyclability. While the surface roughness decreased as a result of the annealing process, the film thickness increased. The annealed WO_3 thin film showed better performance than the as-deposited film with a coloration efficiency of 41.5 $cm^2 \cdot C^{-1}$.

Key words: Tungsten trioxide, Electrochromism, Thin films, Annealing, Ceramics.

Introduction

Electrochromic devices (ECDs) have been widely investigated due to their potential application in smart windows, automobiles, and architectural glazing to result in energy savings [1-4]. ECDs are composed of an electrolyte, an electrochromic layer, an ion storage layer, and a transparent glass substrate with an imposing conductivity. The optical properties of electrochromic devices in the visible range change as a charge is inserted or extracted.

Tungsten trioxide (WO_3) is known as an elec trochromic layer material due to its high coloration efficiency and electrochemical stability compared to other electrochromic materials [5-8]. A number of methods to fabricate WO_3 thin films have been developed including sputtering, sol-gel coating, spray pyrolysis, and electrophoretic deposition [9-14]. Among these, the electrophoretic deposition (EPD) method is very attractive due to its low cost and the formation of homogeneous films. Thus, we adopted electrophoretic deposition for the fabrication of WO_3 thin films [15]. However, the as-deposited WO_3 thin films produced by the EPD process showed degradation after cycling [15]. If the adhesion of WO_3 films to the substrate is not good, the electron transfer could be obstructed and as a result, the electrochromic performance will be degraded. Therefore, an annealing process was introduced in order to improve the adhesion of the as-deposited WO_3 films and improve their elecrochromic properties. The effect of the annealing treatment on the film morphology and electrochromic properties was investigated in this study.

*Corresponding author:
Tel : +82-63-270-2290
Fax: +82-63-270-2386
E-mail: ktlee71@jbnu.ac.kr

Experimental Procedure

The WO_3 precursor sol was prepared by dissolving tungsten metal powder (12 μm, 99.9%, Aldrich) in hydrogen peroxide (30.0-35.5%, Samchun). Per oxotungstic acid (PTA) was synthesized in which chelating [$O2^{2-}$] ligands prevent the formation of an oxide network [16]. The colorless solution of PTA was filtered in order to remove supersaturated tungsten metal powder. Then, the PTA solution was added to a solution of 90/40 v/v water/2-propanol with a pH of 1.8. The prepared coating solution was aged for 48 hrs.

EPD was performed using a DC power supply. A current and voltage of 30 mA and 20 V, respectively, were applied for 180 sec. Pt wire and ITO-coated glass (8.5 ± 1.5 Ω/cm, 185 ± 20 nm) were used as the counter and working electrodes, respectively. The deposited films were thoroughly dried at room temperature and the dried films were calcined at 100 °C for 24 hrs in order to evaluate the annealing effect.

X-ray diffraction was performed using an X-ray diffractometer (Rigaku D/MAX-111A, Japan) with Cu Kα radiation to analyze phases. Diffraction patterns were recorded at a scan rate of 4 °/min in the 2θ range of 20 ° to 80 °. The morphology and thickness of the WO_3 thin films were analyzed by field emission scanning electron microscopy (FE-SEM, S-4800, Hitachi). Raman spectra of the samples were recorded using a high resolution Raman spectrometer (LabRAM, Horiba Jobin-Yvon) equipped with two holographic gratings. The scattered light was detected with a charge-coupled-device (CCD). The excitation source was the 514 nm line of Ar ion laser. The electrochemical properties were evaluated using 1 M LiClO4 in a propylene carbonate electrolyte with a three-electrode

Table 1. Summary of observed and literature data of the Raman for the as-deposited and annealed WO_3 thin films.

Raman shift (cm^{-1})			Peakassignment
As-deposited	Annealed	Reference	
218	220	220 [18]	W^{5+}-W^{5+} or W-W vibrations
679	679	694 [19] 713 [20, 21]	W_2O_6 and W_3O_8 stretching W-O stretching, W-O bending, O-W-O deformation
779	790	790 [22, 23] 807 [20, 21]	W-O-W anti-symmetric stretching W-O stretching, W-O bending, O-W-O deformation
951	953	971 [24]	W = O terminal bond

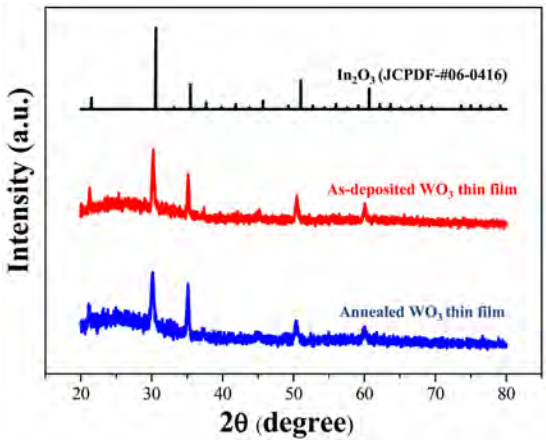

Fig. 1. X-ray diffraction patterns of the as-deposited and annealed WO_3 thin films.

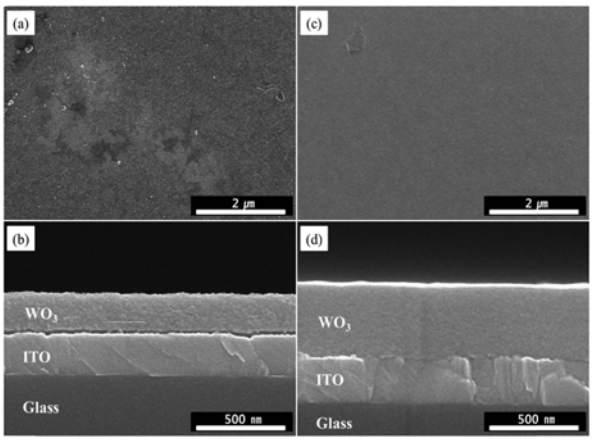

Fig. 2. FE-SEM micrographs of the (a, b) as-deposited WO_3 thin films and (c, d) WO_3 thin films annealed at 100 °C for 24 hrs ((a, c): surface, (b, d): cross section).

electrochemical cell, wherein Ag/AgCl and Pt wires were employed as the reference and counter electrodes, respectively. In-situ transmittance measurements using a He-Ne laser with a wavelength of 632.8 nm were performed during chronocoulometry (CC) at ± 1 V for 180 s. Then, cyclic voltammetry (CV) analysis was carried out in the voltage range of + 1 to −1 V at a scan rate of 20 mV · s^{-1}.

Results and Discussion

X-ray diffraction patterns of the as-deposited and annealedWO3 thin films are shown in Fig. 1. No distinct peaks are detected except ITO peaks. This indicates that the as-deposited WO_3 thin films deposited by the EPD process have amorphous structure. Moreover, the WO_3 thin film annealed at 100 °C for 24 hrs still sustained the amorphous structure.

The morphologies of the as-deposited and annealed WO_3 thin films were observed by FE-SEM, as shown in Fig. 2. Delamination between the WO_3 thin film and ITO layer was observed in the as-deposited sample. This phenomenon may occur during the evaporation of water and iso-propanol. Additionally, the adhesive strength may have weakened due to the insertion/ extraction of protons in the coating solution. On the contrary, the annealed WO_3 film showed better adhesion to the ITO layer compared to the as-deposited film. Interestingly, the film thickness increased and

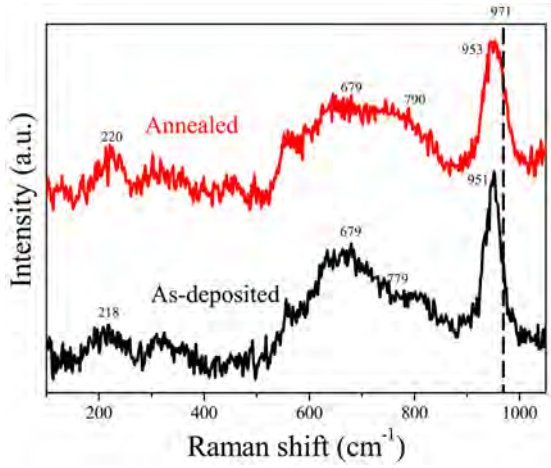

Fig. 3. Raman spectra of the as-deposited and annealed WO_3 thin films.

surface roughness decreased as a result of the annealing process. The annealing process may cause residual stress relaxation resulting in volume expansion. Raman spectroscopy can analyze mechanical properties of thin films such as stress and strain [17].

Fig. 3 shows the Raman spectra of the as-deposited and annealed WO_3 films. The assignment and comparison of the characteristic vibrations of the Raman spectra are given in Table 1. All peaks are well matched with the previous reports. Typically, Raman peaks of the transition metal (M) oxide in the range

Table 2. Electrochromic properties of the as-deposited and annealed WO_3 thin films for the first cycle.

Sample	$T_{bleached}$ (%)	$T_{colored}$ (%)	ΔT (%)	Charge density ($mC \cdot cm^{-2}$)	Coloration efficiency ($cm^2 \cdot C^{-1}$)
As-deposited	84.5	60.1	24.4	5.1	28.7
Annealed	94.3	10.1	84.2	23.4	41.5

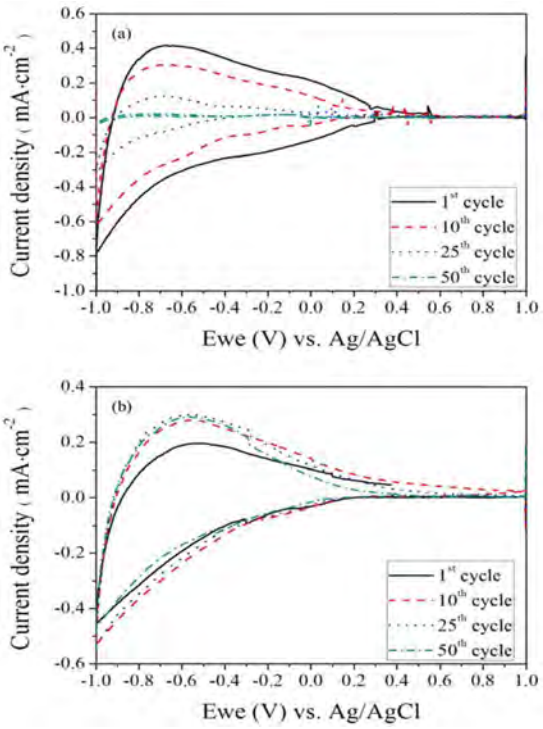

Fig. 4. Cyclic voltammogram of the (a) as-deposited WO_3 thin films and (b) WO_3 thin films annealed at 100 °C for 24 hrs.

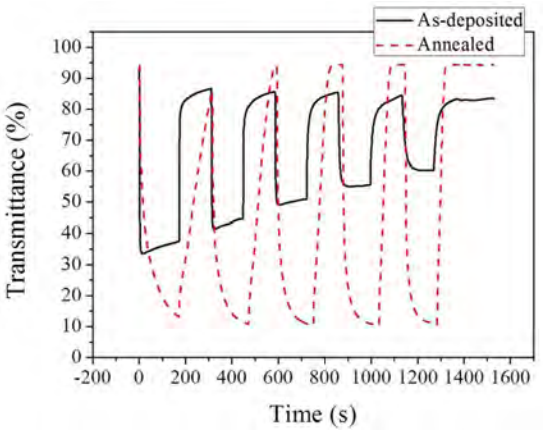

Fig. 5. Transmittance measurement data of the as-deposited and annealed WO_3 thin films.

950-1050 cm^{-1} can be assigned to a symmetric stretching mode of short terminal M = O bands. Therefore, the peak at 971 cm^{-1} is the fingerprint peak to characterize the WO_3 thin film. It has been reported the Raman peak position shifts to higher wavenumbers with the increase of compressive stress and it shifts to lower wavenumbers with the increase of tensile stress [25]. The fingerprint peak in Fig. 3 shifted to lower wave number from the reference, which indicates that the WO_3 thin films deposited by the EPD process have a tensile stress. The annealed film showed relatively less shift compared to the as-deposited film. Considering the residual stress and the Raman peak position shifts before and after annealing, it can be concluded that annealing process may relax the tensile stress in the WO_3 thin film. Meanwhile, the intensities of the reference peaks at 790 cm^{-1} and 807 cm^{-1} compared with the fingerprint peak at 971 cm^{-1} indicate the crystallinity of WO_3 thin film [26]. The intensities of the peaks at 679 cm^{-1} and 790 cm^{-1} increased after the annealing process as shown in Fig. 3. Although the WO_3 thin films deposited by the EPD process showed amorphous structure in the long-range order by X-ray diffraction analysis as shown in Fig. 1, it may show an increase in crystallinity in the short-range order by the annealing process.

Fig. 4 shows the CV data of the as-deposited and annealed WO_3 thin films. While the cathodic peak current density of the as-deposited WO_3 thin film decreased significantly with increasing cycle number, the cathodic peak current density of the annealed WO_3 thin film increased and maintained its initial value even at the 50th cycle. The cathodic peak current density is proportional to the capacity of Li ion insertion, which is strongly related to the electron transfer between the electrochromic and electrode layers. The crack between the WO_3 thin film and the ITO layer shown in Fig. 2could interrupt the electron transfer, consequently leading to the significant degradation with cycling. Finally, the as-deposited WO_3 films were peeled off after the cycling test. The initial cathodic peak current density of the as-deposited WO_3 thin film was higher than that of the annealed film. This result is attributed to the surface roughness of the WO_3 thin films. The Li ion insertion/extraction reaction depends on the number of reaction sites on the surface as well as electron transfer. The as-deposited WO_3 thin film with a rough surface has a large amount of reaction sites compared to the annealed film. Therefore, the as-deposited WO_3 thin film exhibited a higher cathodic peak current density than the annealed film.

The optical properties of the as-deposited and annealed WO_3 thin films are shown in Fig. 5. The colored and bleached states of the WO_3 thin films were achieved by reduction at −1 V and oxidation at + 1 V vs. Ag/AgCl, respectively. The transmittance variation (ΔT) of the as-deposited WO_3 thin film decreased

significantly with cycling. The variation of ΔT demonstrated the same behavior as the CV data trends, as shown in Fig. 4. The response time tbleached (or tcolored) for bleaching (or coloring) of the WO_3 thin films is defined as the time interval between the highest and lowest variation rates in transmittance. In other word, the steep slope between bleaching and coloring states indicates fast response time. As shown in Fig. 3, the response time of the annealed WO_3 film became faster than the initial value as the cycle number increased.

Based on the data in Fig. 5, the calculated electrochromic properties for the first cycle are listed in Table 2. The annealed WO_3 thin film had a larger transmittance variation value than the as-deposited film, which can be explained by the film thickness. The colored states occur as a result of lithium insertion andthe thick WO_3 film is able to hold a relatively large amount of lithium. Therefore, the thick WO_3 film annealed at 100 ºC for 24 hrs showed the largest transmittance variation.

The coloration efficiency (CE) is one of the most important parameters and is often used to characterize electrochromic materials [27].

$$CE = \frac{\Delta OD}{q/A} = \frac{1}{q/A} \bullet log\left[\frac{T_{bleached}(\%)}{T_{colored}(\%)}\right] \quad (1)$$

Here, ΔOD is the change in the optical density normalized by the number of charges intercalated per the unit electrode area, A is the area of the electrode, q is the electric charge, and $T_{bleached}$ and $T_{colored}$ are the transmittances of the film in the bleached and colored states, respectively. A greater CE corresponds to a greater transmittance variation per unit charge. The annealed WO_3 thin film showed better performance than the as-deposited film with a coloration efficiency of 41.5 $cm^2 \cdot C^{-1}$.

Conclusions

WO_3 thin films were fabricated by an EPD process and the effects of annealing on the film morphology and electrochromic properties were investigated. The surface of the as-deposited WO_3 thin films became smooth and the film thickness increased after the annealing process. Thicker WO_3 filmscan hold a large amount of Li ions. Moreover, adhesion between the WO_3 film and ITO glass was enhanced by annealing, which led to an improvement of the electron transfer. Consequently, the annealed WO_3 thin film exhibited a better electrochromic property and cyclability than the as-deposited film.

Acknowledgments

This research was financially supported by the Ministry of Knowledge Economy (MKE) and Korea Institute for Advancement of Technology (KIAT) through the Research and Development for Regional Industry.

References

1. C.G. Granqvist, A. Azens, A. Hjelm, L. Kullman, G.A. Niklasson, D. Ronnow, M.S. Mattsson, M. Veszelei, G. Vaivars, Sol. Energy. 63 (1998) 199-216.
2. C.G. Granqvist, P.C. Lansker, N.R. Mlyuka, G.A. Niklasson, E. Avendano, Sol.Energ. Mat. Sol. C 83 (2009) 2032-2039.
3. A. Georg, A. Gerog, Sol. Energ. Mat. Sol. C 93 (2009) 1329-1337.
4. N. Sbar, M. Badding, R. Budziak, K. Cortez, L. Laby, L. Michalski, T. Ngo, S. Schulz, K. Urbanik, Sol. Energ. Mat. Sol. C 56 (1999) 321-341.
5. R. Baetens, B.P. Jelle, A. Gustavsen, Sol.Energ. Mat. Sol. C 94 (2010) 87-105.
6. K.K. Purushothanman, G. Muralidharan, J. Sol-gel Sci.Tech. 46 (2008) 190-194.
7. S.J. Yoo, J.W. Lim, Y.E. Sung, Sol. Energ. Mat. Sol. C 90 (2006) 477-484.
8. R. Hurditch, Electrocomp. Sci. Tech. 3 (1977) 247-251.
9. T.S. Tung, L.C. Chen, K.C. Ho, Solid State Ionics. 165 (2003) 257-267.
10. K. Yamanaka, H. Oakamoto, H. Kidou, T. Kudo, Jpn. J. Appl. Phys. 25 (1986) 1420-1426.
11. P.D. Davidse, Vacuum. 17 (1976) 139-145.
12. H. Kawasaki, T. Matsunaga, W. Guan, T. Ohshima, Y. Yagyu, Y. Suda, J. Plasma Fusion Res. 8 (2009) 1431-1434.
13. A.K. Chawla, S. Singhal, H.O.Gupta, R. Chandra, Thin Solid Films. 518 (2009) 1430-1433.
14. D.J. Taylor, J.P. Cronin, L.F. Allard Jr., D.P. Birnie, Chem. Mater. 8 (1996) 1396-1401.
15. Y.T. Park, K.T. Lee, J. Ceram. Proc. Res. 13 (2012) 607-611.
16. Z. Wang, X. Hu, Electrochim. Acta. 46 (2001) 1951-1956.
17. G. Gouadec, P. Colomban, Prog. Cryst. Growth Charact. Mater. 53 (2007) 1-56.
18. S.H. Lee, H.M. Cheong, C.E. Tracy, A. Mascarenhas, D.K. Benson, S.K. Deb, Electrochim. Acta. 44 (1999) 3111-3115.
19. W. Weltner, D. Mcleod, J. Mol. Spect. 17 (1965) 276-299.
20. P. Tagtstrom, U. Jansson, Thin Solid Films. 352 (1999) 107-133.
21. G.A. de Wijs, R.A. de Groot, Electrochim. Acta. 46 (2001) 1989-1993.
22. B.M. Weckhuysen, J.M. Jehng, I.E. Wachs, J. Phys. Chem. B 104 (2000) 7382-7387.
23. J. Nagai, Electrochim. Acta. 46 (2001) 2049-2053.
24. M. Regragui, M. Addou, A. Outzourhi, J.C. Bernede, E. El Idrissi, E. Benseddik, A. Kachouane, Thin Solid Films. 358 (2000) 40-45.
25. P.C. Liao, C.S. Chen, W.S. Ho, Y.S. Huang, K.K. Tiong, Thin Solid Films. 301 (1997) 7-11.
26. K. Yamanaka, H. Oakamoto, H. Kidou, T. Kudo, Jpn. J. Appl. Phys. 25 (9) (1986) 1420-1426.
27. M. Deepa, A.K. Srivastava, K.N. Sood, S.A. Agnihotry, Appl. Surf. Sci. 252 (2005) 1568-1580.